Title: A head-fixation system for continuous monitoring of force generated during behavior

Authors: Ryan N. Hughes[1], Konstantin I. Bakhurin[1], Joseph W. Barter[1], Jinyong Zhang[1], Henry H. Yin[1,2*]

Affiliations:

[1]Department of Psychology and Neuroscience, Duke University, Durham, NC, 27708, USA.,

[2]Department of Neurobiology, Duke University School of Medicine, Durham, NC, 27708, USA.

*Correspondence to: **hy43@duke.edu**

Abstract

Many studies in neuroscience use head-fixed behavioral preparations, which confer a number of advantages, including the ability to limit the behavioral repertoire and use techniques for large-scale monitoring of neural activity. But traditional studies using this approach use extremely limited behavioral measures, in part because it is difficult to detect the subtle movements and postural adjustments that animals naturally exhibit during head fixation. Here we report the development of an apparatus that is equipped with analog load cells capable of precisely monitoring the continuous forces exerted by mice. The load cells reveal the dynamic nature of movements generated not only around the time of task-relevant events, such as the regular presentation of stimuli and rewards, but also during periods of no apparent overt behavior that occur outside of the experimenter-defined events. It generates a new and rich set of behavioral measures that have been neglected in previous experiments. We detail the construction of the system, which can be 3D-printed and assembled at low cost (~$140), show behavioral results collected from head-fixed mice, and demonstrate that neural activity can be highly correlated with the subtle, whole-body movements continuously produced during head restraint.

Introduction

Many studies in modern behavioral neuroscience use head-fixation (Toda et al., 2017;Coddington and Dudman, 2018;Economo et al., 2018). Historically, head-fixed experimental preparations in awake behaving animals have contributed to the study of motor control (Evarts, 1968;Hikosaka and Wurtz, 1983), associative learning (Waelti et al., 2001;Eshel et al., 2015), and even navigation (Dombeck et al., 2010). Head-fixation confers two major advantages. First, it allows convenient monitoring of neural activity that minimizes noise and motion artifact. This enables the use of powerful techniques for recording neural activity on a large scale, such as two-photon calcium imaging or electrophysiology using large electrode arrays. Second, by greatly constraining the behaviors that the animal can perform, it simplifies experimental design and data analysis. For this reason, studies using head-fixation usually focus on the behavior of interest. The typical measures used include licking, EMG measures of arm or mouth muscle activity, bar pressing, and eye movements (Newsome et al., 1989;Schultz et al., 1992;Eshel et al., 2015;Economo et al., 2018). While these measures have provided valuable insights, other behaviors generated by the head-fixed animals are neglected. For example, many postural adjustments of the body are not measured. Researchers often assume that no other behaviors, such as head movements, are occurring. However, just because these subtle movements cannot be easily observed, it does not follow that there are no attempts to move the head or other body movements. Furthermore, often animals are placed in chambers or rooms away from the experimenter, so that close observation of the actual behavior is not even attempted. Because neural activity recorded during standard behavioral tasks could well be related to the generation of such movements, they produce significant confounding variables. The lack of knowledge of such variables can therefore result in misinterpretation of neural activity while the true relationships between neural activity and behavior is overlooked.

More recent systems have attempted to address some of these concerns by incorporating a running ball for continuous locomotion in head-fixed animals (Dombeck et al., 2010;Engelhard et al., 2019). During such experiments, animals often make direction-specific adjustments of the body and the head, in addition to their limb movements, in order to steer the ball appropriately. However, the coordinate (x, y, and z) positions of the ball provide little information about the actual kinematics of the body. Others have incorporated accelerometers into their head-fixation devices, thus allowing measurements of whole-body movements (Coddington and Dudman, 2018). The major limitation of accelerometer baskets is they cannot distinguish between movements in different directions, as movements in any direction can result in the same accelerometer reading. Moreover, head movements are not usually measured.

Here we describe a novel head-fixation apparatus equipped with load cells for detection of forces generated by the head and body in head-fixed mice. The system uses multiple sensors to continuously monitor not only the magnitude but also direction of forces that result from head movements as animals move and adjust their posture while head-fixed. The apparatus reveals the subtle movements that are continuously generated by head-fixed animals, even during the performance of simple behavioral tasks that are used in these preparations.

Results

To quantify direction-specific and continuous movements in the head-fixed preparation, we developed a novel head-fixation device that incorporates 5 load cells to directly measure the forces generated by the mice's head and body movements (Figure 1A, for detailed instructions on assembling the device, see the Materials and Methods section "Assembly Instructions").

Mice are implanted with a steel head post as part of routine surgery to implant electrodes into the brain. The post is secured into the apparatus by small pinch clamps, which are part of a lightweight, rectangular plastic frame. The frame is suspended by an array of 3 aluminum load cells, which simultaneously register the forces exerted by the animal in 3 directions (Figures 1A & 1B).

This precise arrangement of load cells suspending the mouse's head enabled the measurement of independent force vectors along orthogonal axes of movement (up/down, left/right, or forward/backward). The load-cells are arranged in a tight cluster together just above the mouse to avoid spurious measures of torque as well as to capture as much of the individual force vector as possible. Two additional sensors were placed below the left and right feet in a custom-designed perch (Figure 1B), in order to measure the forces exerted by each side of the body as the mouse adjusts its posture. All components of the head-fixation device were custom-designed and 3-D printed in the lab.

Small strain gauge load cells designed to operate on a scale of 0-100g were used. Load cells of this type and size are most commonly found in small weighing devices such as kitchen scales. Attached to the aluminum body of the load-cell are sensitive strain gauges arranged in a Wheatstone bridge configuration (Figure 2A). Changes in the shape of the bridge can alter its resistance and voltage levels across the gauges. Because the load-cells register changes to the shape of their aluminum bodies, the cluster of 3 load cells that support the head-fixation frame acts as the frame's pivot-point as it slightly moves along 3-dimensions in response to the mouse's movement. The voltage between the Wheatstone bridges is modulated by deformations of the strain gauges, which is proportional to the amount of force exerted. The load cell is coupled to an amplifier circuit that scales this voltage between 0 and 5V, which can be used by

most analog recording systems (Figure 2A). The configuration of the circuit shown is designed to detect bidirectional forces exerted on the load cell. The load cell signal is linearly proportional to the amount of force applied to it in either direction (Figure 2B). By measuring the slope between known masses and the voltage reading, one can convert the measured voltage to force applied to the load cell. By using a low-resistance trimmer potentiometer between pins 8 and 9 in the amplification circuit, it allows the user to adjust the slope of the voltage change in response to changes in force.

Behavior on a fixed-time reinforcement schedule

We tested our load-cell head-fixation device using 2 mice chronically implanted with a head bar. Mice began training on a fixed-time (FT) schedule of reinforcement where they received a 10% sucrose solution every 10 seconds (Figure 3A). During early sessions in the fixed-time task, mice will readily collect water from the spout, but have not yet begun to time the arrival of this drop (Figure 3A). Our system was able to detect the fine and subtle movements during the task. For a given single trial, force exertion was predominantly coincident with their licking behavior after reward delivery, reflecting forward movements towards the spout (Figures 3B & 3G). However, their movements from side to side were different, with one mouse showing large rightward movements and the other showing large leftward movements following the reward (Figures 3C & 3H). Both mice showed a movement upward as they collected the reward (Figures 3D & 3I). However, the reason for their movement upward can be inferred by examining the measurements from the force sensors below the feet. One mouse clearly pressed down with both feet (Figures 3E & 3F) to collect the reward, whereas another mouse preferentially applied force with the left side of its body (Figures 3J & 3K). The signals

registered by each load cell were distinct for a given trial, reflecting the complexity and amplitude of coordinated movements generated by different parts of the body (Figures 3B-L). In addition, our system could quantify unique movement patterns in each mouse, even when they are engaged in an extremely simple behavioral task.

Well-trained mice (approximately 1-2 weeks) initiated licking prior to reward presentation (Figure 3A). Similar to what was observed early in training, movements closely coincided with licking. However, after training, both the licking and force measures started before reward delivery (Figure 4). Although both mice displayed stereotyped anticipatory licking before reward (Rossi and Yin, 2015;Rossi et al., 2016;Toda et al., 2017), their movements and postural adjustments were both complex and unique. Licking-related oscillations were nested within slower-frequency movements that reflected positional and postural changes of the whole body. However, our force measures reveal that, even though the licking becomes stereotyped as the task is learned, the movements from trial-to-trial remain highly variable. In a single reward trial, one mouse displayed forward movements along with large amplitude leftward movements during both anticipatory licking and licking following reward (Figures 4A & 4B). In contrast, the other mouse displayed backward movements and rightward movements during both anticipatory and consummatory licking (Figures 4G & 4H). Both mice showed upward forces while they licked (Figures 4C & 4I). The foot sensors revealed that these upward movements were due to pushing down onto the floor of the perch (Figures 4D, 4E, 4J, & 4K). Although the dynamics of these movements were complex, we found that generally the largest exertion of force by both mice was along the forward/backward and side-to-side dimensions (Figures 4F & 4L).

Neural recordings of VTA activity while measuring whole body movement forces in head-fixed mice

The dynamic force signals detected by the load-cells reflect subtle changes in movement of the head and posture of the body that vary from one trial to another. We therefore asked whether such continuous measures of movement are related to neural activity. Neurons in the VTA have recently been demonstrated to control the angular position of the head in three-dimensional space (Hughes et al., 2019). To determine whether VTA activity is related to forces in the head-fixation system, we recorded single unit activity from the VTA of well-trained mice performing the fixed-time task (n = 2, Figure 5A), isolating spiking activity from putative GABAergic neurons in this region.

As was observed in the single-trial examples (Figures 3 & 4), the force signals that we measured tended to coincide with licking behavior. To reveal the variability of these movements across many trials, we aligned the neural activity of a putative GABAergic neuron to reward and then sorted both the force measures and the neural data by the latency to the first lick following reward (Figures 5B & 5C). This approach revealed striking patterns between the neural data, licking, and movements of the whole body in the head-restrained mice. An examination of all the force sensor raster plots revealed high trial-to-trial variability when aligned to reward, even in well-trained mice. At the same time, the signals revealed a remarkable coordination as the mice anticipated and consumed the reward, likely reflecting the whole-body movements produced by the head-restrained mouse (forward, leftward, and downward movements; Figures 5D-H). The single unit activity was highly correlated with the movements (Figure 5P). We observed a similar pattern in a second neuron (Figure 5I) from a different mouse. In this example, the mouse moved forward, leftward, and upward, pushing down with both feet while consuming the reward

(Figures 5 J-O). Interestingly in this example, the load cells could register an oscillatory signal in the mouse's movements during reward consumption, which was most likely due to oscillations from extension and retraction of the tongue (Figures 5J & 5K). Remarkably, this was largely reflected in the activity of the isolated single unit (Figure 5I). This feature is again rendered unintelligible using the average activity across trials.

These preliminary results reveal the importance of recording the continuous movement of mice when they are head restrained. The simultaneous acquisition of both neural data and continuous kinematic measure of the head and body demonstrates that the neural activity more closely corresponds to the animals' continuous movements, rather than to the events defined and imposed by the experimenter. Indeed, we found high correlations of the neural activity with load sensor signals (Figure 5P). Importantly, these correlation values indicate that neurons can have selectively high relationships for specific directions of movement.

Behavior during Pavlovian conditioning

Many studies in head-fixed mice employ Pavlovian conditioning approaches to study learning and to isolate specific goal-directed behaviors (Figure 6A, left). Virtually no study has examined the head movements or body forces exerted by head-fixed mice during such tasks. To demonstrate the utility of our device for these kinds of studies, we recorded VTA activity from two different well-trained mice performing a standard Pavlovian trace conditioning task (Figure 6A, right). During this task, mice received a 5 µl drop of sucrose (US) that was preceded by a 100-millisecond tone (CS) separated by a 1 second delay. Trials were separated by random inter-trial intervals (3-60 seconds). We simultaneously recorded neural activity and the forces exerted (Figures 6B-E). In this task, the mice displayed two phases of force exertion: a large movement immediately following reward and more subtle movements that occurred following the tone

presentation (Figures 6B & 6D). Significantly, when we sorted the trials according to force initiation, the neural activity often closely followed the force changes, though each neuron that we recorded from showed distinct relationships to movements during each event (Figures 6B-E). Two neurons predominantly responded to movements following the tone (Figure 6C), and an additional two cells were sensitive to movements generated following the tone and following reward (Figure 6E). Importantly, averaging the neural activity only conveyed the responses of neurons to movements following reward, but did not reveal the relationships that these neurons had to movements following the tone. Only by examining individual trials and sorting the data according to the mice's behavior were these significant relationships revealed. Thus, the preliminary results with our experimental setup demonstrate that there are valuable behavioral measurements besides licking that can be taken during head-fixation tasks.

Discussion

One major limitation in behavioral neuroscience research is the lack of precise, continuous and direction-specific behavioral measurements. Head-fixation has attempted to overcome these limitations by allowing investigators to focus their analysis on a subset of movements with fine precision. Our results contradict the common misconception that additional movements of the body and head are irrelevant once mice are head restrained. For convenience, these behaviors are usually neglected in traditional neuroscience experiments. We have shown that ignoring these movements can severely limit our understanding of brain function. Our device reveals that even during head fixation, animals are often making many continuous adjustments of the head and body while performing a given task. Furthermore, we show that

neural activity can be closely aligned with these movements of the body, revealing a new dimension of explanatory variables for complex neural data.

Although head-fixation facilitates our ability to understand neural activity by providing precise measures of some behaviors such as licking or eye movements, our device shows that there are many movements of the head and body that are occurring during head-fixation even though they are never explicitly measured. These head and body movements often occur simultaneously with the traditional measures such as licking (Figures 3 & 4) and therefore cause an important movement confound in all past research using head-fixation. In addition, the strain put on the skull from trying to move the head while clamped to a rigid structure presents an unavoidable source of significant and highly variable sensory input due to the sensory feedback from the movements themselves. Therefore, two major confounds exist in previous studies using head-fixed approaches while investigating the neural substrates of a given behavior. If these considerations are not taken into account, it is easy to slip into accounting for activity patterns in the nervous system by ascribing the brain with unnecessarily complex and arbitrary functions.

Even a behavior as simple as eating a piece of food entails coordinating multiple muscle effectors with a variety of perceptual variables (e.g. jaw, neck, arm and tongue muscles being coordinated in relation to the distance of the piece of food to the mouth). The time courses and dynamics of these variables are likely to be quite distinct for every individual piece eaten. This trial-to-trial variability in motor output can render averaging neural data and behavior across mice highly ambiguous and misleading. We show that mice make many head and body movements during the performance of traditional head-fixation tasks, and their neural activity can follow these dynamics quite closely (Figures 3-6). Thus, many studies claiming to investigate the neural correlates of variables such as reward or value during head-fixed studies

have failed to notice a large movement confound. It would be helpful to reexamine all previous head-fixed studies using continuous force measures as introduced here.

One possible reason these variables have not been taken seriously is that the traditional approach is based on experimenter-defined behavioral events, rather than continuous processes (Yin, 2017). Actions are often assumed to be 'all-or-none' discrete events, such as reaching, licking, button pressing, or saccades. Behavior is thus only quantified as a categorical time stamp, rather than as a continuous process which unfolds over time. As a result, investigators have only attempted to understand neural activity by aligning it to this observer-defined action and analyzing its activity around this time point. The neural activity that occurs in between experimenter-defined events is usually disregarded as noise. Our system demonstrates that, with continuous behavior measures, neural activity outside of these observed defined time-points becomes quite structured, and clear relationships can be found that demonstrate it is not noise or artifact.

Variability in neural activity has long been a puzzle for neuroscience (Shadlen and Newsome, 1998;Osborne et al., 2005). The results obtained from our novel head-fixation device point towards a potential source of this variability: continuous behavior that has not been noticed or measured. By aligning the force measures and neural activity to experimenter-defined events, but sorting the trials according to continuous behavioral measures, the neural activity outside of these events is revealed to reflect the continuous force measures and not the events. Without such measures, averaging neural activity around discrete events produces interference of these structured signals, which causes the neural activity to appear as noise. Our device thus reveals the potential source of this 'noise' in nervous system activity (Figures 5 & 6). Importantly, our

results demonstrate that it is not noise but meaningful neural activity that needs to be explained by any theory of the brain.

While newer head-fixed set ups utilize a running ball or an accelerometer in order to measure the behavior of the mouse, there are several disadvantages associated with these setups (Harvey et al., 2009;Coddington and Dudman, 2018). First, it is impossible to detect direction-specific adjustments of the head and body with either an accelerometer basket or a running ball. Second, the coordinates and the speed of the ball are only indirect measures of the actual kinematics. Furthermore, the treadmill ball has its own momentum that can be independent of the animal's movement. For example, if the ball is moving to the left, but the mouse wants to go forward, many opposing adjustments of the limbs and body have to occur to counteract the ball's momentum in order to provide forward motion. The measures from the ball could indicate a turn from left to forward whereas the mice are making large adjustments in different directions in order to obtain the new heading.

Our head-fixation system addresses these problems by directly and continuously measuring the forces exerted by the mouse's head as well as the forces exerted by both sides of the body. The chief advantages of our design are its low-cost (~$140; see materials and methods for parts list and price), ease of construction, and its precise, direction-specific measurements of the mice's head and body. This is accomplished by increasing the number of sensors that we are able to record from. In contrast to other methods that attempt to measure movement during head-fixation (Coddington and Dudman, 2018), this system was designed to confront the fact that the head is the primary point of stress and contact that the behaving mouse has with the restraining system. Our head-fixation system can be used in conjunction with treadmills balls to detect these adjustments, where the direction-specific head movements can be measured and directly

compared with the coordinates obtained from the ball. This would make it possible to dissociate head movements and limb movements.

To further our understanding of how the nervous system generates behavior, behavior must be continuously measured with high temporal and spatial resolution. Only then can behavior be adequately related to the corresponding neural activity (Figures 4-5).

Methods

Mice: All experimental procedures were approved by the Mouse Care and Use Committee at Duke University. Four C57BL/6J mice between 2-6 months old were used for experiments (Jackson Labs, Bar Harbor, ME). Mice were housed in groups of 3-4 mice per cage on a 12:12 light cycle, with experiments conducted during the light phase. During days where mice were run on experiments, they were water restricted and maintained at 85-90% of their initial body weights. Mice received free access to water for approximately 2 hours following the daily experimental session.

Load Cells and Circuit: Each load cell (RobotShop, Swanton, VT, USA) is a full Wheatstone bridge with a configuration of four balanced resistors based on a known excitation voltage, as shown below:

$$V_f = (R_3R_3 + R_4 - R_2R_1 + R_2)V_{EX}$$

Where R is the resistor, V_{EX} is a known constant excitation voltage, and output V_f is variable depending on the shape of the strain gauge. Thus, a bidirectional sensing amplifier connected to the load cell will output 2.5V at zero load. When the load is increased or decreased, the voltage will correspondingly increase or decrease. In other words, if the load is positive, voltage output

will increase, and if the load is negative, voltage will decrease. This relationship is described by the following:

$$V_f = 2.5V + [(V_{IN}^{+} - V_{IN}^{-})\ (4 + \frac{60k\Omega}{Rg})]$$

Where Rg is the resistance of the potentiometer, k is the cell sensitivity and V_{IN} is the voltage coming from the load cell. We also attached a potentiometer to the circuit. The sensitivity of the circuit can be adjusted using the potentiometer, which is a precise trimmer potentiometer with 200 Ohms resistance. We used a high accuracy amplifier (INA125UA, Texas Instruments) chip, which has a precision voltage reference. The amplifier gain (Gf) from this chip is described as below.

$$G_f = 4+60k/R_g$$

The voltage obtained from the amplifier (INA125UA) is then linearly correlated with the force on the load cell. That means we can use the voltage to describe the force exerted on each orthogonal load cell. From Newton's second law ($F = ma$, where F = force, m = mass and a = acceleration), a mass with a known quantity placed on the load cell can be multiplied by gravity in order to obtain a force-voltage conversion factor (F/V). This conversion factor can then be used to convert the voltage signal to a force that is being exerted on the load cell. The resistance values for load cells used for behavioral experiments were: 103 Ohms (F/B force sensor); 102.5 Ohms (S/S Force sensor); 103 Ohms (U/D force sensor); 102.8 Ohms (right feet force sensor); 103.1 Ohms (left feet force sensor).

Head-fixed behavioral setup: The apparatus was 3D printed in PLA plastic using a MakerGear M2 3D printer (MakerGear, Beachwood, OH, USA). Both mouse perch and head fixation apparatus were bolted to a steel base plate (Thorlabs, Newton, NJ, USA), and elevated to give sufficient space for the reward delivery apparatus. In the floor of the perch, two 100g load cells (RobotShop, Swanton, VT, USA) were used to measure ground reaction forces on the left and right side of the mice. The mice's head implants were clamped to a custom frame that was suspended above them. In the head fixation apparatus between the point of head fixation and the base plate, three 100g load cells of the same type were arranged orthogonally to detect force changes in three dimensions (forwards-backwards, up-down, and left-right). These load cells were connected in series and arranged close together and in line with the mouse's head to minimize twisting forces. Each load cell was connected by a shielded cable to an amplifier circuit, which was in turn connected to the data acquisition system. Each load cell signal was recorded continuously as an analog voltage. Load cells translate mechanical stress caused by an applied load into a voltage signal. We amplified the signal using an INA125UA (Texas Instruments; http://www.mechtechplace.net/mech-tech-electronics/building-a-low-cost-strain-gage-load-cell-amplifier/). Proper grounding of the circuit is important, as it can introduce noise into electrophysiological and force sensor recordings. A 10 % sucrose solution gravity-fed from a reservoir was delivered to the mice via a metal spout placed in close proximity to their mouth. Sucrose delivery was controlled through the use of a solenoid valve (161T010, NResearch, NJ). A capacitance-touch sensor (MPR121, AdaFruit.com) was clamped to the metal spout in order to record licking behavior. All analog voltage signals (1 Khz) and electrophysiological data were recorded using a Blackrock Cerebrus recording system (Blackrock Microsystems) for offline

analysis. Electrical noise that appeared in force sensor signals was removed in post-processing in some sessions.

Assembly Instructions:

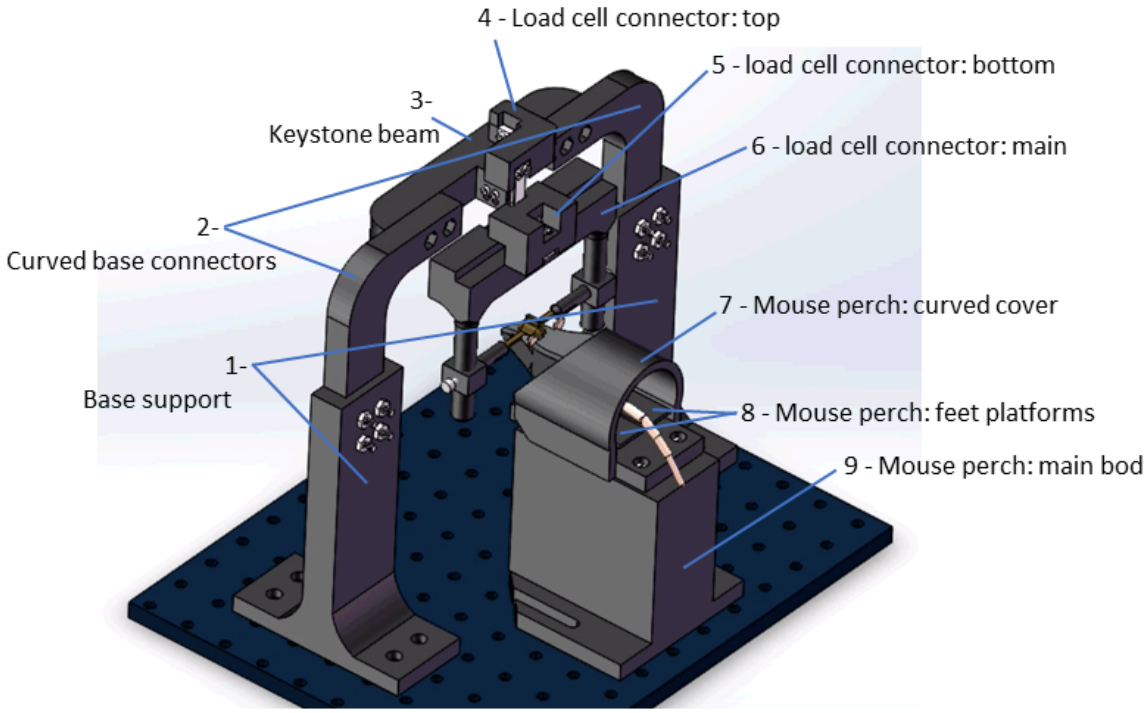

Instructions for assembling the head fixation apparatus:

1) Attach base supports (parts 1) to the steel baseplate using M6 bolts.

2) Attach curved base connectors (parts 2) to base support (parts 1) using M6 nuts and bolts.

3) Attach keystone beam (part 3) to base connectors (parts 2) using M6 nuts and bolts.

4) Attach the lower end of a load cell to keystone beam (part 3) using M2.5 bolts.

5) Attach the upper end of the load cell to the thin side of top load cell connector (part 4) using M2.5 bolts.

6) Attach the upper end of a second load cell to the thick side of the top load cell connector (part 4) using M2.5 bolts.

7) Attach bottom load cell connector (part 5) to the lower end of the second load cell using M2.5 bolts.

8) Attach a third load cell to main load cell connector (part 6) using M2.5 bolts.

9) Attach the other side of the third load cell to bottom load cell connector (part 5) using M2.5 bolts.

Instructions for assembling the perch apparatus:

1) Attach fourth and fifth load cells side by side to the inside of the curved cover of the mouse perch (part 7) using M2.5 bolts.

2) For both the fourth and fifth load cell, attach the free end to a copy of the platforms of the mouse perch (parts 8) using M2.5 bolts. The flat side of feet platforms of the mouse perch (parts 8) should face upward.

3) Attach the curved cover of the mouse perch (part 7) to the main body of the mouse perch (part 9) using M6 bolts. Attachment holes in part 9 should be self-threading.

4) Attach the main body of the mouse perch (part 9) to the steel baseplate using M6 bolts through the attachment channels at the base of the main body of the mouse perch (part 9).

*See supplemental video S1 and S2 for a 3D rendering of construction.

Parts list:

1) Spool of 3D printer filament. Any rigid plastic works. We used PLA on Fused deposition modeling (FDM) printer (1x $18.00 per spool, https://www.amazon.com/SUNLU-Filament-1-75mm-Printer-Black/dp/B07Q82HVTT/ref=sr_1_14?keywords=PLA+filament&qid=1579894242&s=industrial&sr=1-14).

2) 100g load cell (5x, $7.00 each, https://www.robotshop.com/en/100g-micro-load-cell.html?gclid=EAIaIQobChMIybPxse2c5wIVzJ-zCh353gR0EAQYBSABEgJbLvD_BwE).

3) INA125 Instrumentation Amplifier (5x, ~$7.00 each, https://www.digikey.com/product-detail/en/texas-instruments/INA125UA/INA125UA-ND/300986).

4) Trimmer potentiometer (5x, $1.36 each, https://www.digikey.com/product-detail/en/nidec-copal-electronics/ST4ETB101/ST4ETB101CT-ND/738511).

5) 4 pin male connector (5x, $0.4 each, https://www.digikey.com/product-detail/en/1718560004/WM10155-ND/4423111/?itemSeq=314595070).

6) 4 pin female connector (5x, $0.45 each, https://www.digikey.com/product-detail/en/PPTC041LFBN-RC/S7002-ND/810144/?itemSeq=314595184).

7) 2 pin male connector (6x, $0.2 each, https://www.digikey.com/product-detail/en/0022280020/WM19475-ND/3157814/?itemSeq=314595790).

8) Jumper wires assortment (1x, $7.29 each,https://www.amazon.com/Yueton-Multicolored-Female-Breadboard-Jumper/dp/B01DDD1LXU/ref=sr_1_25?keywords=jumper+wires&qid=1579893448&s=hi&sr=1-25)

9) 3-conductor shielded cable for connecting load cells to amplifier circuits (~$60 for 3.05m, https://www.digikey.com/product-detail/en/alpha-wire/85243CY-BK005/85243CYBK005-10-ND/9090384)

10) M6 nuts and bolts assortment (1x, $19.50, https://www.amazon.com/120Pcs-Stainless-Socket-Washers-Assortment/dp/B01N0ZU46G?ref_=fsclp_pl_dp_15)

11) M2.5 bolts assortment (1x, $9.99, https://www.amazon.com/HVAZI-Stainless-Phillips-Machine-Assortment/dp/B075QKZ8PY/ref=sr_1_7?keywords=m2.5+bolts&qid=1579890750&s=hi&sr=1-7)

12) Printed circuit board (1x, ~$3.00 per board, depending on supplier and quantity).

Wireless in Vivo *Electrophysiology:* Mice were anesthetized with 2.0 to 3.0% isoflurane, then placed into a stereotactic frame (David Kopf Instruments, Tujunga, CA) that was maintained at 1.0 to 1.5 % isoflurane for surgical procedures, as previously described(Fan et al., 2011;Fan et al., 2012). A craniotomy was then made above the VTA. Fixed 16-channel electrodes (Innovative Neurophysiology, Inc.) were lowered into the VTA (AP: 3.2 mm, ML 0.5 mm, DV, -4.2 mm) through the craniotomy. Electrode arrays were composed of tungsten electrodes in a 4 x 4 configuration (35 μm diameter, 150 μm spacing, 5 mm length). After electrodes were inserted, they were secured to the skull using screws and dental acrylic, followed by the insertion of a metal bar around the dental acrylic to allow for head-fixation (Toda et al., 2017).

Behavioral tasks: Mice were allowed to recover for 2 weeks, then mice (n = 2) were trained on a fixed time (FT) reinforcement schedule for approximately 1-2 weeks (Rossi et al., 2013;Toda et

al., 2017). An additional 2 mice were trained on a trace Pavlovian conditioning task for approximately 5-7 days until anticipatory licking was observed after the sound of the tone. The tone lasted 100 ms, followed by a 1 second delay. Reward was then delivered after the delay. A random ITI of 3-60 seconds was used in between reward trials. A miniaturized wireless head stage (Triangle Biosystems) that communicated with a Cerebrus data acquisition system (Blackrock Microsystems) was used to record electrophysiological data (Fan et al., 2011;Barter et al., 2014). All single unit data were then sorted offline using OfflineSorter (Plexon). All plots for electrophysiological and force signal data were created with NeuroExplorer (Nex Technologies) using 50 ms bins. In order to be included for analysis, neural data must have had a 3:1 signal-to-noise ratio, with an 800 μs or greater refractory period.

Acknowledgments: This study was supported by NIH grants NS094754, DA040701, and MH112883 to HHY. We would like to dedicate this paper to the memory of Kobe Bryant (1978-2020), whose artistry and dedication have been a major source of inspiration.

Figure legends

Fig. 1. **Novel head-fixation set up measures force of the head in 3 orthogonal directions and left and right body forces**

A) Illustration of novel head-fixation apparatus with five orthogonal force sensors from the front (*left*), side (*middle*) and back (*right*). There are three force sensors that measure the force exerted by the mice's head (1, 2 and 3). Two additional force sensors are below the mice's feet on the left and right side of the body (4 and 5). For further instructions, see methods section on assembling the device. **B**) Schematic representation of each force sensors and the direction of force that it measures. Force sensor 1 measures force made by the head in the forwards and backwards direction. Force sensor 2 measures force made by the head in the side-to-side (left and right) direction. Force sensor 3 measures force made by the head in the upward and downward direction. Force sensors 4 and 5 measure force exerted in the upward and downward direction made by the right and left feet, respectively

Fig. 2. **Load cell circuit and set up allows for data acquisition with any device that can read an analog signal**

A) Circuit diagram for the load cell. The load cell is attached to an amplifier that contains a potentiometer. This allows the user to adjust the slope of the load cell voltage output in response to force changes in order to tune it for the optimal linear relationship between voltage and the force applied to the load cell. From this circuit, the voltage output is then connected to a data acquisition system to collect continuous voltage signal data. Inset shows the printed circuit board (PCB) designed for 5 load cells. **B**) There is a linear relationship between mass applied to the

load cell and the change in voltage output. By using an object with a known mass, a mass-voltage relationship can be obtained using different levels of resistance from the potentiometer. From Newton's second law ($F = ma$), the known mass can be multiplied by gravity in order to obtain a force-voltage conversion factor (F/V) in order to obtain the force exerted on the load cell.

Fig. 3. **Force sensors detect continuous and fine movements of the head and body during early training in a fixed time (FT) behavioral task**

A) Two mice were trained on a fixed-time schedule of reinforcement where they received a 10% sucrose solution every 10 seconds. **B-F)** Raw continuous traces of 10 seconds from all five force sensors, as well as lick times, obtained from mouse 1. Each force sensor displays distinct force changes that vary in their amplitude and direction. **G-K)** Raw continuous traces of 10 seconds from all five force sensors, as well as lick times, obtained from mouse 2. **L**) Average peak forces exerted for each force sensor across all trials from both mice.

Fig. 4. **Movements measured by force sensors remain variable even when licking becomes stereotyped when the FT task is well-learned** **A-E)** Raw continuous traces of 10 seconds from all five force sensors, as well as lick times, obtained from mouse 1. Each force sensor displays distinct force changes that vary in their amplitude and direction. **G**) Average peak forces exerted for each force sensor across all trials from mouse 1. **G-K)** Raw continuous traces of 10 seconds from all five force sensors, as well as lick times, obtained from mouse 2. **G**) Average peak forces exerted for each force sensor across all trials from mouse 2.

Fig. 5. **Neural data and precise force measurements can be used to find relationships between neural activity and behavior in head-fixed set ups.**

A) An electrode was implanted into the VTA (n = 2). Waveform of typical putative VTA GABAergic neuron shown on right. **B**) Representative putative GABAergic neuron aligned to the onset of licks after reward from mouse 1. Trials were sorted according to the initiation of the first lick. **C**) Corresponding licks from the same behavioral session. **D-H)** Data from all 5 force sensors aligned to the onset of licks after reward (mouse 1). Color bars on the right of the heatmaps indicate the amplitude and direction of movement in the heatmap (F = forward, B = Backward, L = Left, R = Right U = Up, D = Down) **I**) Representative putative GABAergic neuron aligned to the onset of licks after reward from mouse 2. **J**) Corresponding licks from the same behavioral session. **K-O)** Data from all 5 force sensors aligned to the onset of licks after reward (mouse 2). P) Correlation values

Fig. 6. **Characteristic force measures and neural activity on a Pavlovian conditioning task.**

A) Mice were trained on a Pavlovian trace conditioning task where a 100 ms tone (CS) was presented, followed by a 1 second delay and the delivery of a 10 % sucrose reward (US). There was a random interval trial interval (ITI) of 3-60 seconds. **B)** Head force measures showing mice exert large head forces during the task. **C)** Two corresponding representative putative GABAergic neurons from the VTA of mouse 3. Trials are sorted according to the start of the first forward movement. **D)** Head force measures during the

task. **E)** Two corresponding representative putative GABAergic neurons from the VTA of mouse 4. Trials are sorted according to the start of the first forward movement.

References

Barter, J.W., Castro, S., Sukharnikova, T., Rossi, M.A., and Yin, H.H. (2014). The role of the substantia nigra in posture control. *European Journal of Neuroscience* 39 (9)**,** 1465-1473.

Coddington, L.T., and Dudman, J.T. (2018). The timing of action determines reward prediction signals in identified midbrain dopamine neurons. *Nature neuroscience* 21**,** 1563.

Dombeck, D.A., Harvey, C.D., Tian, L., Looger, L.L., and Tank, D.W. (2010). Functional imaging of hippocampal place cells at cellular resolution during virtual navigation. *Nat Neurosci* 13**,** 1433-1440.

Economo, M.N., Viswanathan, S., Tasic, B., Bas, E., Winnubst, J., Menon, V., Graybuck, L.T., Nguyen, T.N., Smith, K.A., Yao, Z., Wang, L., Gerfen, C.R., Chandrashekar, J., Zeng, H., Looger, L.L., and Svoboda, K. (2018). Distinct descending motor cortex pathways and their roles in movement. *Nature* 563**,** 79-84.

Engelhard, B., Finkelstein, J., Cox, J., Fleming, W., Jang, H.J., Ornelas, S., Koay, S.A., Thiberge, S.Y., Daw, N.D., Tank, D.W., and Witten, I.B. (2019). Specialized coding of sensory, motor and cognitive variables in VTA dopamine neurons. *Nature***,** 1.

Eshel, N., Bukwich, M., Rao, V., Hemmelder, V., Tian, J., and Uchida, N. (2015). Arithmetic and local circuitry underlying dopamine prediction errors. *Nature* 525**,** 243-246.

Evarts, E.V. (1968). Relation of pyramidal tract activity to force exerted during voluntary movement. *Journal of neurophysiology* 31**,** 14-27.

Fan, D., Rich, D., Holtzman, T., Ruther, P., Dalley, J.W., Lopez, A., Rossi, M.A., Barter, J.W., Salas-Meza, D., Herwik, S., Holzhammer, T., Morizio, J., and Yin, H.H. (2011). A wireless multi-channel recording system for freely behaving mice and rats. *PLoS One* 6**,** e22033.

Fan, D., Rossi, M.A., and Yin, H.H. (2012). Mechanisms of action selection and timing in substantia nigra neurons. *J Neurosci* 32**,** 5534-5548.

Harvey, C.D., Collman, F., Dombeck, D.A., and Tank, D.W. (2009). Intracellular dynamics of hippocampal place cells during virtual navigation. *Nature* 461**,** 941-946.

Hikosaka, O., and Wurtz, R.H. (1983). Visual and oculomotor functions of monkey substantia nigra pars reticulata. III. Memory-contingent visual and saccade responses. *J Neurophysiol* 49**,** 1268-1284.

Hughes, R.N., Watson, G.D., Petter, E.A., Kim, N., Bakhurin, K.I., and Yin, H.H. (2019). Precise Coordination of Three-Dimensional Rotational Kinematics by Ventral Tegmental Area GABAergic Neurons. *Current Biology*.

Newsome, W.T., Britten, K.H., and Movshon, J.A. (1989). Neuronal correlates of a perceptual decision. *Nature* 341**,** 52-54.

Osborne, L.C., Lisberger, S.G., and Bialek, W. (2005). A sensory source for motor variation. *Nature* 437**,** 412-416.

Rossi, M.A., Fan, D., Barter, J.W., and Yin, H.H. (2013). Bidirectional Modulation of Substantia Nigra Activity by Motivational State. *PloS one* 8**,** e71598.

Rossi, M.A., Li, H.E., Lu, D., Kim, I.H., Bartholomew, R.A., Gaidis, E., Barter, J.W., Kim, N., Cai, M.T., Soderling, S.H., and Yin, H.H. (2016). A GABAergic nigrotectal pathway for coordination of drinking behavior. *Nat Neurosci*.

Rossi, M.A., and Yin, H.H. (2015). Elevated dopamine alters consummatory pattern generation and increases behavioral variability during learning. *Front Integr Neurosci* 9**,** 37.

Schultz, W., Apicella, P., Scarnati, E., and Ljungberg, T. (1992). Neuronal activity in monkey ventral striatum related to the expectation of reward. *J Neurosci* 12**,** 4595-4610.

Shadlen, M.N., and Newsome, W.T. (1998). The variable discharge of cortical neurons: implications for connectivity, computation, and information coding. *J Neurosci* 18**,** 3870-3896.

Toda, K., Lusk, N.A., Watson, G.D.R., Kim, N., Lu, D., Li, H.E., Meck, W.H., and Yin, H.H. (2017). Nigrotectal Stimulation Stops Interval Timing in Mice. *Curr Biol* 27**,** 3763-3770 e3763.

Waelti, P., Dickinson, A., and Schultz, W. (2001). Dopamine responses comply with basic assumptions of formal learning theory. *Nature* 412**,** 43-48.

Yin, H.H. (2017). The Basal Ganglia in Action. *Neuroscientist* 23.

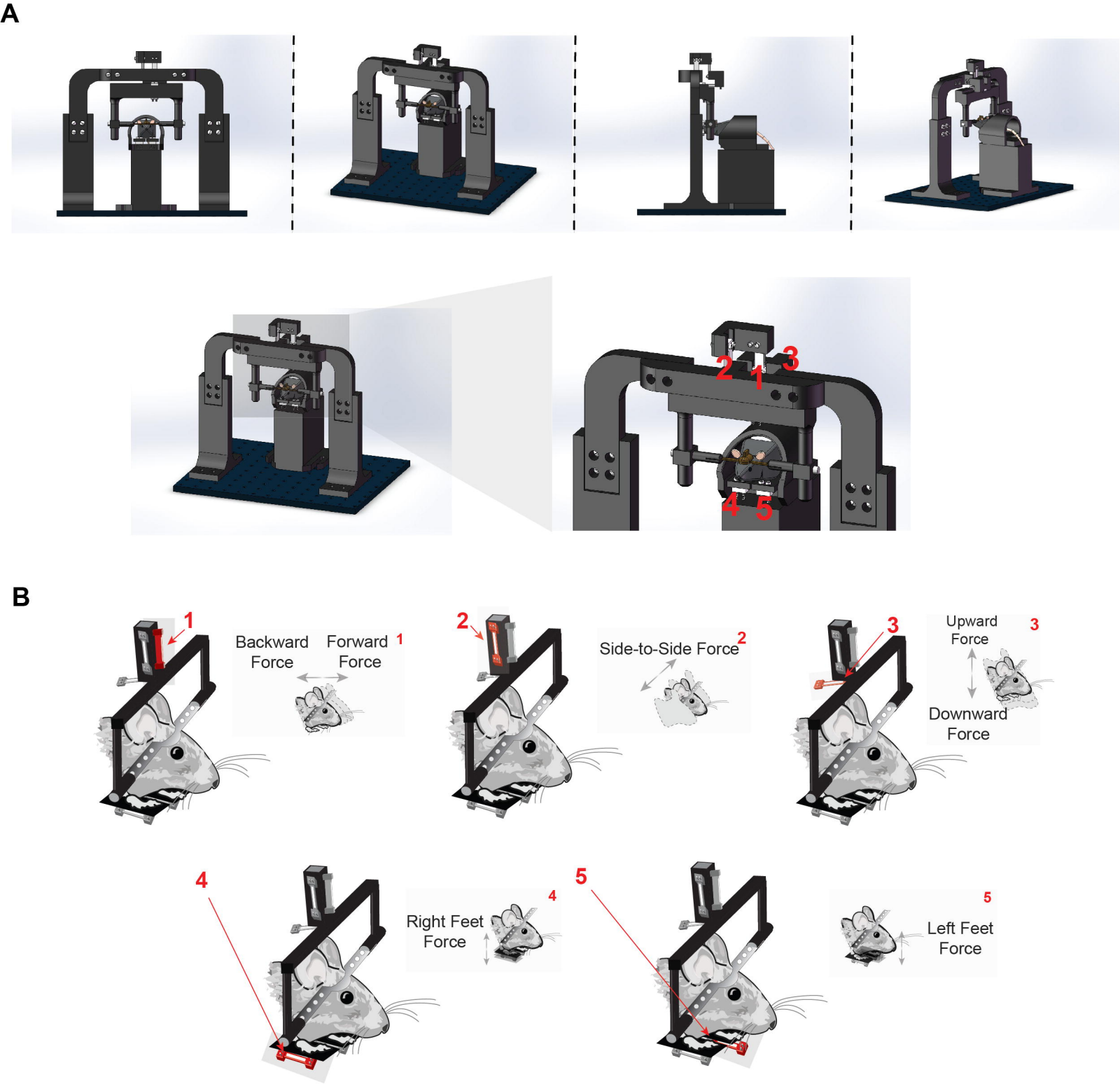
A
1
2
3
4
5
B
1
Backward Force
Forward Force
2
Side-to-Side Force
3
Upward Force
Downward Force
4
Right Feet Force
5
Left Feet Force

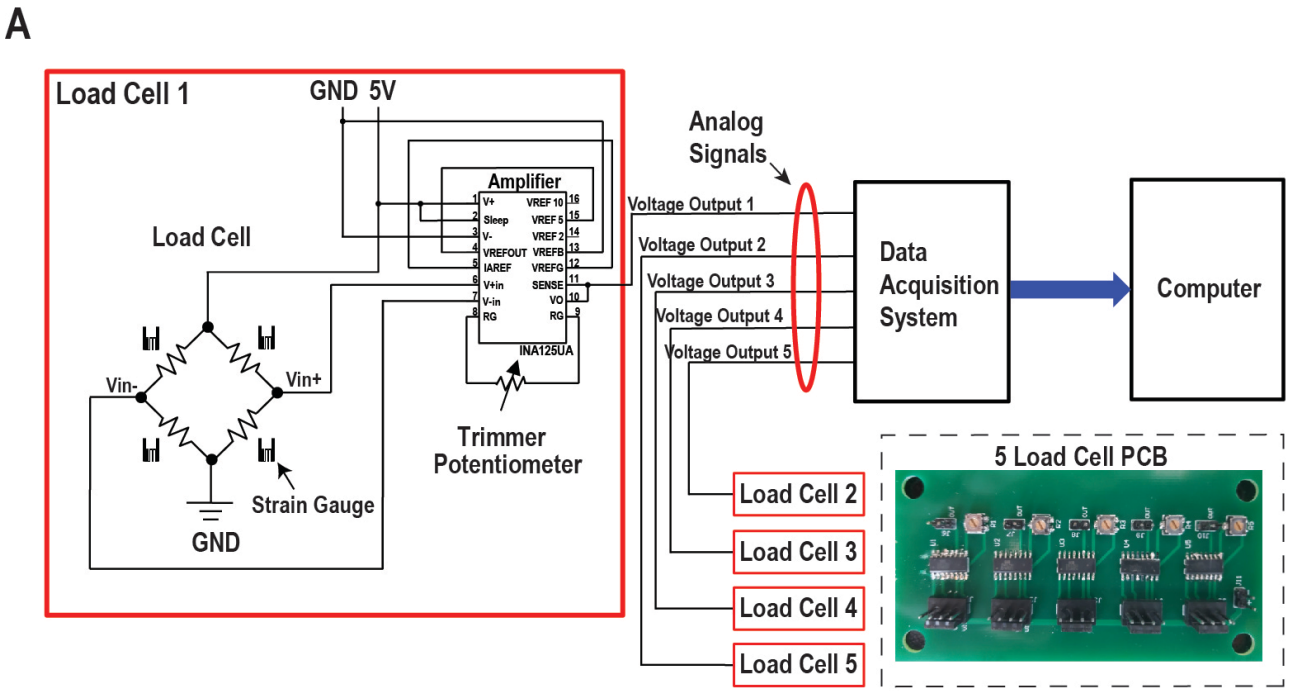

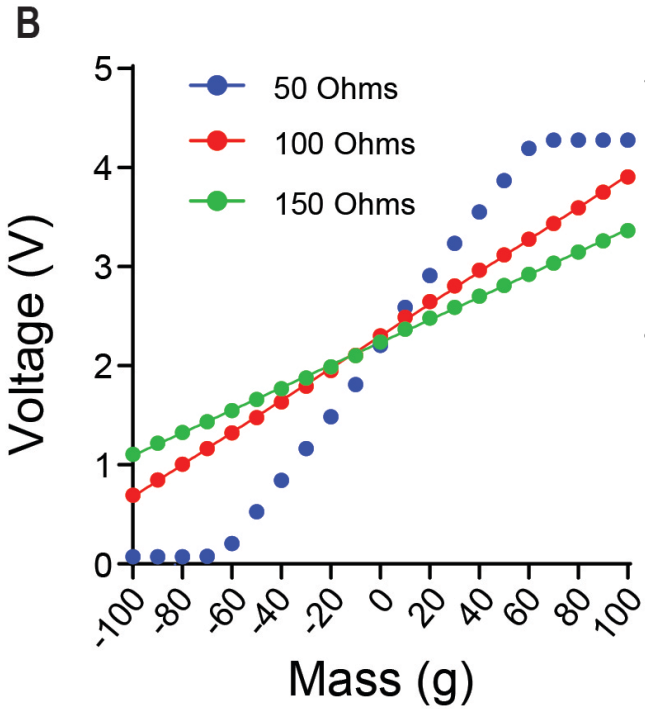

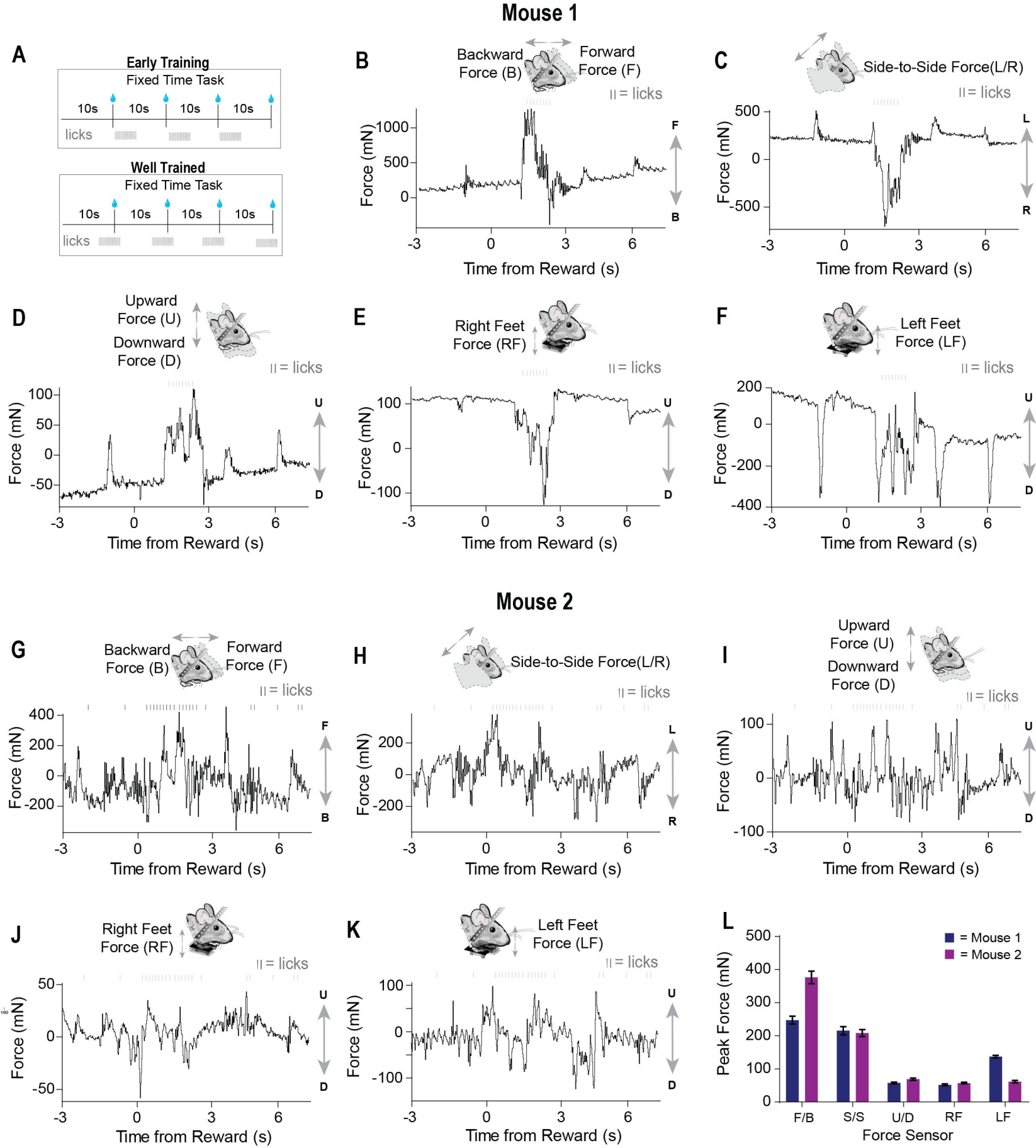
Mouse 1
A
Early Training
Fixed Time Task
10s
10s
10s
10s
licks
Well Trained
Fixed Time Task
10s
10s
10s
10s
licks
B
Backward
Force (B)
Forward
Force (F)
= licks
Force (mN)
1000
500
0
F
B
-3
0
3
6
Time from Reward (s)
C
Side-to-Side Force(L/R)
= licks
Force (mN)
500
0
-500
L
R
-3
0
3
6
Time from Reward (s)
D
Upward
Force (U)
Downward
Force (D)
= licks
Force (mN)
100
50
0
-50
U
D
-3
0
3
6
Time from Reward (s)
E
Right Feet
Force (RF)
= licks
Force (mN)
100
0
-100
U
D
-3
0
3
6
Time from Reward (s)
F
Left Feet
Force (LF)
= licks
Force (mN)
200
0
-200
-400
U
D
-3
0
3
6
Time from Reward (s)
Mouse 2
G
Backward
Force (B)
Forward
Force (F)
= licks
Force (mN)
400
200
0
-200
F
B
-3
0
3
6
Time from Reward (s)
H
Side-to-Side Force(L/R)
= licks
Force (mN)
200
0
-200
L
R
-3
0
3
6
Time from Reward (s)
I
Upward
Force (U)
Downward
Force (D)
= licks
Force (mN)
100
0
-100
U
D
-3
0
3
6
Time from Reward (s)
J
Right Feet
Force (RF)
= licks
Force (mN)
50
0
-50
U
D
-3
0
3
6
Time from Reward (s)
K
Left Feet
Force (LF)
= licks
Force (mN)
100
0
-100
U
D
-3
0
3
6
Time from Reward (s)
L
= Mouse 1
= Mouse 2
Peak Force (mN)
500
400
300
200
100
0
F/B
S/S
U/D
RF
LF
Force Sensor

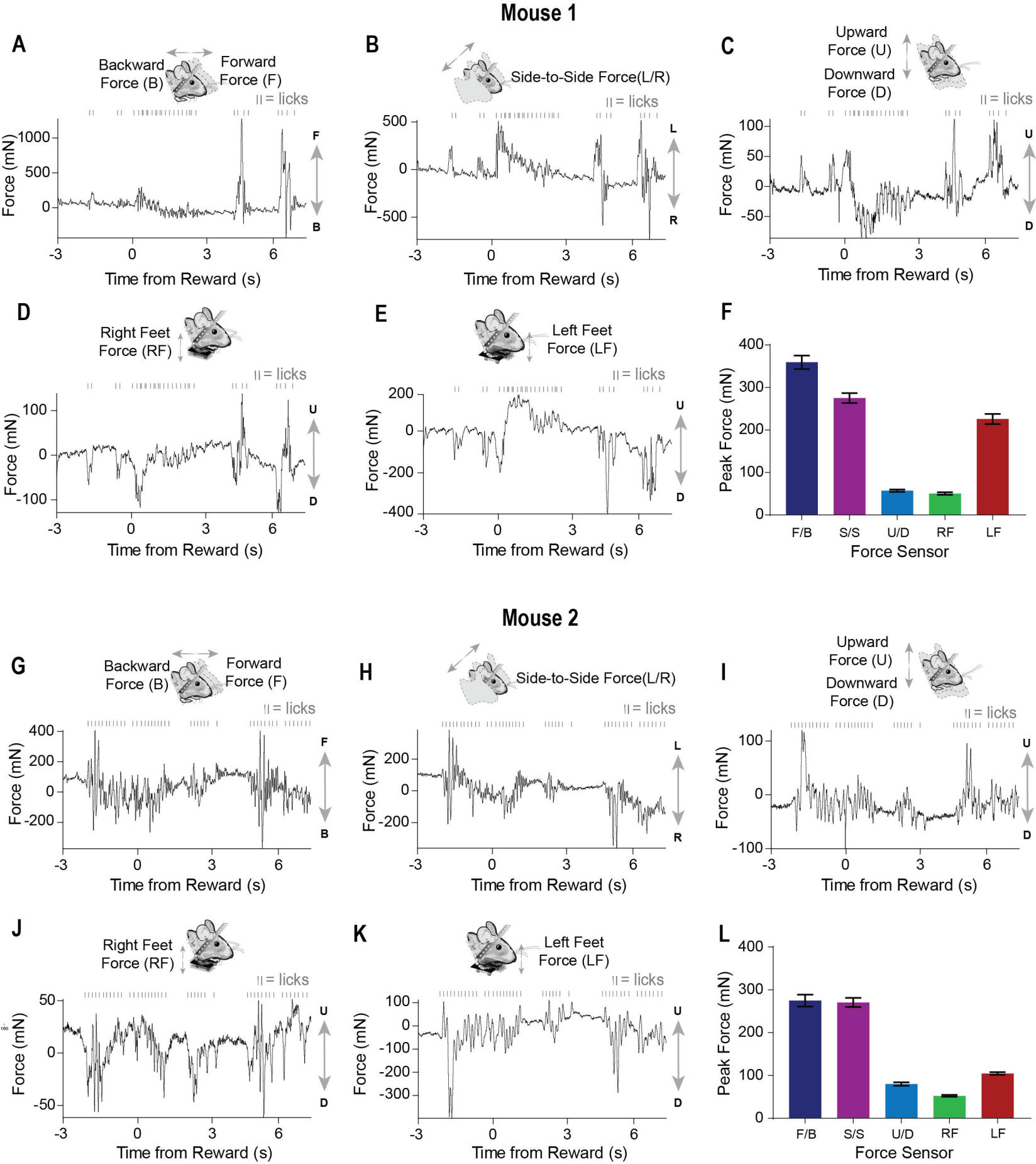
Mouse 1
A
Backward Force (B)
Forward Force (F)
|| = licks
Force (mN)
1000
500
0
F
B
-3
0
3
6
Time from Reward (s)
B
Side-to-Side Force(L/R)
|| = licks
500
0
-500
L
R
Force (mN)
Time from Reward (s)
C
Upward Force (U)
Downward Force (D)
|| = licks
100
50
0
-50
U
D
Force (mN)
Time from Reward (s)
D
Right Feet Force (RF)
|| = licks
100
0
-100
U
D
Force (mN)
Time from Reward (s)
E
Left Feet Force (LF)
|| = licks
200
0
-200
-400
U
D
Force (mN)
Time from Reward (s)
F
400
300
200
100
0
Peak Force (mN)
F/B
S/S
U/D
RF
LF
Force Sensor
Mouse 2
G
Backward Force (B)
Forward Force (F)
|| = licks
400
200
0
-200
F
B
Force (mN)
Time from Reward (s)
H
Side-to-Side Force(L/R)
|| = licks
200
0
-200
L
R
Force (mN)
Time from Reward (s)
I
Upward Force (U)
Downward Force (D)
|| = licks
100
0
-100
U
D
Force (mN)
Time from Reward (s)
J
Right Feet Force (RF)
|| = licks
50
0
-50
U
D
Force (mN)
Time from Reward (s)
K
Left Feet Force (LF)
|| = licks
100
0
-100
-200
-300
U
D
Force (mN)
Time from Reward (s)
L
400
300
200
100
0
Peak Force (mN)
F/B
S/S
U/D
RF
LF
Force Sensor

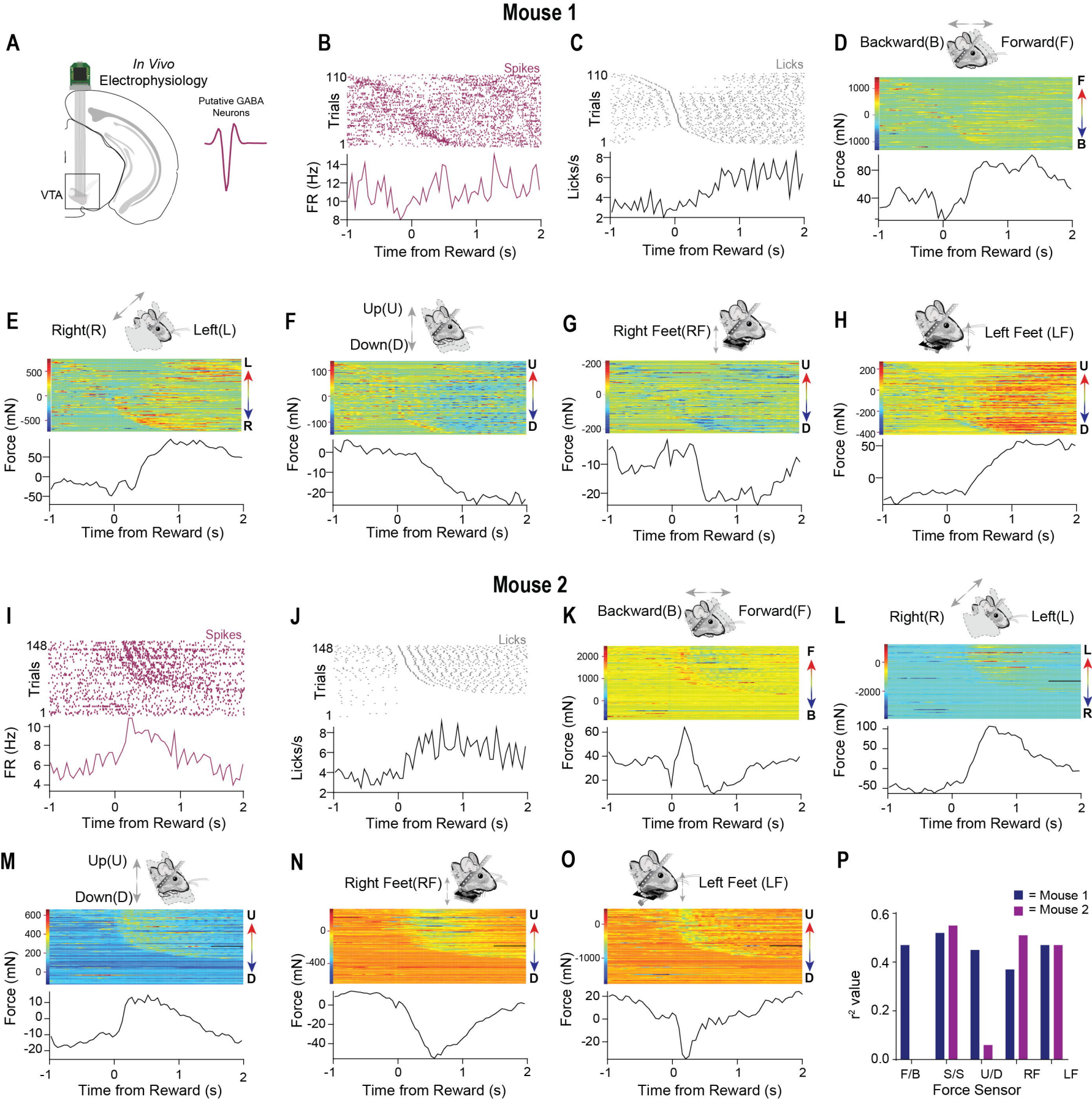
Mouse 1
A
In Vivo
Electrophysiology
Putative GABA
Neurons
VTA
B
Spikes
Trials
FR (Hz)
Time from Reward (s)
C
Licks
Licks/s
D
Backward(B)
Forward(F)
Force (mN)
E
Right(R)
Left(L)
F
Up(U)
Down(D)
G
Right Feet(RF)
H
Left Feet (LF)
Mouse 2
I
J
K
L
M
N
O
P
= Mouse 1
= Mouse 2
r² value
F/B
S/S
U/D
RF
LF
Force Sensor

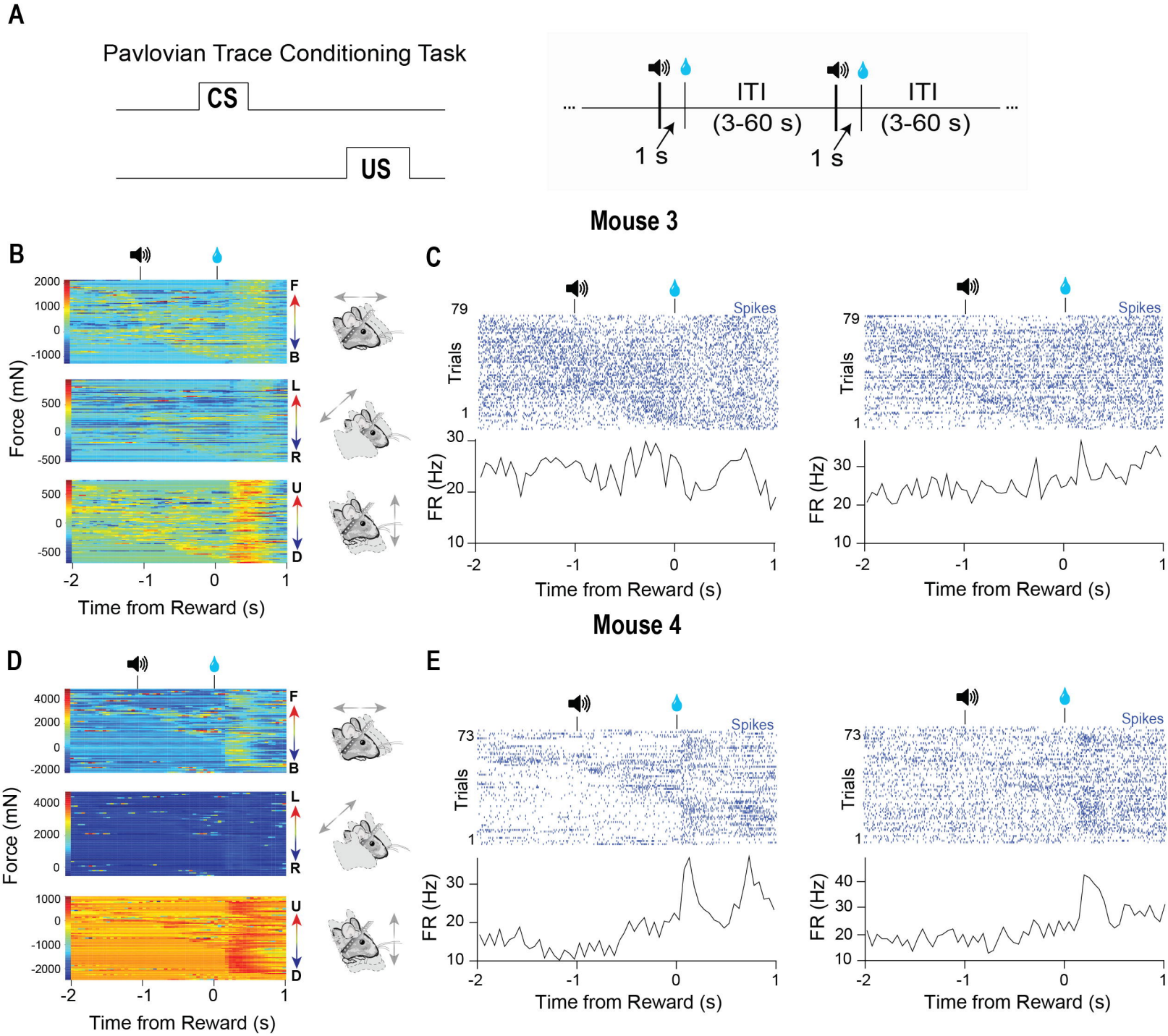
A
Pavlovian Trace Conditioning Task
CS
US
ITI
(3-60 s)
1 s
ITI
(3-60 s)
1 s
Mouse 3
B
Force (mN)
Time from Reward (s)
C
Spikes
Trials
FR (Hz)
Time from Reward (s)
Mouse 4
D
Force (mN)
Time from Reward (s)
E
Spikes
Trials
FR (Hz)
Time from Reward (s)